# Oligopolyphenylenevinylene-Conjugated Oligoelectrolyte Membrane Insertion Molecules Selectively Disrupt Cell Envelopes of Gram-Positive Bacteria

Jamie Hinks,[a] Wee Han Poh,[a] Justin Jang Hann Chu,[b] Joachim Say Chye Loo,[a,c] Guillermo C. Bazan,[d] Lynn E. Hancock,[e]
[iD] Stefan Wuertz[a,f,g]

Singapore Centre on Environmental Life Sciences Engineering (SCELSE), Nanyang Technological University, Singapore, Singapore[a]; Laboratory of Molecular RNA Virology and Antiviral Strategies, Department of Microbiology, Yong Loo Lin School of Medicine, National University Health System, National University of Singapore, Singapore, Singapore[b]; School of Materials Science and Engineering, Nanyang Technological University, Singapore, Singapore[c]; Department of Chemistry & Biochemistry and Materials, Center for Polymers and Organic Solids, University of California, Santa Barbara, California, USA[d]; Department of Molecular Biosciences, University of Kansas, Lawrence, Kansas, USA[e]; School of Civil and Environmental Engineering, Nanyang Technological University, Singapore, Singapore[f]; Department of Civil and Environmental Engineering, University of California, Davis, California, USA[g]

The modification of microbial membranes to achieve biotechnological strain improvement with exogenous small molecules, such as oligopolyphenylenevinylene-conjugated oligoelectrolyte (OPV-COE) membrane insertion molecules (MIMs), is an emerging biotechnological field. Little is known about the interactions of OPV-COEs with their target, the bacterial envelope. We studied the toxicity of three previously reported OPV-COEs with a selection of Gram-negative and Gram-positive organisms and demonstrated that Gram-positive bacteria are more sensitive to OPV-COEs than Gram-negative bacteria. Transmission electron microscopy demonstrated that these MIMs disrupt microbial membranes and that this occurred to a much greater degree in Gram-positive organisms. We used a number of mutants to probe the nature of MIM interactions with the microbial envelope but were unable to align the membrane perturbation effects of these compounds to previously reported membrane disruption mechanisms of, for example, cationic antimicrobial peptides. Instead, the data support the notion that OPV-COEs disrupt microbial membranes through a suspected interaction with diphosphatidylglycerol (DPG), a major component of Gram-positive membranes. The integrity of model membranes containing elevated amounts of DPG was disrupted to a greater extent by MIMs than those prepared from *Escherichia coli* total lipid extracts alone.

Oligopolyphenylenevinylene-conjugated oligoelectrolytes (OPV-COEs) are a recently described class of membrane insertion molecules (MIMs) that target the microbial envelope with the specific aim of promoting charge transfer across microbial membranes and which potentially have a range of other biotechnological applications (1, 2). OPV-COEs are amphipathic molecules consisting of a conjugated benzene ring backbone that is terminated with ionic pendant chains that have an affinity for biological membranes because of the charge distribution and amphiphilic nature of the molecule (see Fig. 1). The molecular length of the OPV-COE can be tuned by changing the number of phenylenevinylene units in the backbone, and structural modification of the aromatics can confer a range of properties. For example, fluorination of the central aromatic ring dramatically alters the electrostatic distribution along the aromatic backbone and the hydrophobic and electrostatic interactions that drive aggregation (3). Modifying the physicochemical nature of biological membranes in order to stimulate desirable features of microbial metabolism using MIMs represents a conceptual departure from current research efforts and is an interesting biotechnological innovation. This emerging field of research, which includes improving charge transfer across microbial membranes and the fortification of the lipid bilayer to counter solvent stress, is currently underexplored, and the technical scope of membrane-modifying MIMs is not yet fully appreciated. Little is understood about OPV-COE interactions at the cellular level; accordingly, opportunities for discovery in this expanding field exist.

Traditionally, MIMs have attracted research interest because of their antimicrobial properties. The predominant antimicrobial

mechanism of the cationic peptide magainin, an archetype antimicrobial MIM derived from frogs' skin, lies in its ability to disrupt the natural order of biological membranes, causing pores to form in what typically is regarded as a lethal mechanism common to many MIMs (4, 5). The microbial membrane represents a barrier between the cytoplasm and the environment, and a porated membrane reduces the cell's ability to maintain osmotic control, which causes cells to die or curtails their growth (5, 6). Because OPV-COEs, which are essentially MIMs designed for biotechnological purposes, interact with the microbial membrane, it is reasonable to expect that they have the potential to disrupt normal membrane function as well as to enhance it. Therefore, there exists a requirement to characterize the extent to which OPV-COEs perturb microbial membranes.

A recent molecular dynamics study demonstrated a gradient of

membrane perturbation caused by OPV-COE insertion into *Escherichia coli* membranes ranging from moderate, where cells are still viable and can divide, to fatal (3). The degree of membrane perturbation is correlated with particular molecular features, with the primary determinant of membrane perturbation being the molecular length of the MIM. The more closely the molecular length of the MIM matched the thickness of the phospholipid bilayer, the lower the degree of membrane perturbation (3, 7). The mechanism suggested for membrane perturbation was the pinching together of the inner and outer leaflets of the phospholipid bilayer by the shorter MIMs. The extent of the hydrophobic mismatch between the molecular length of the MIM and the bilayer thickness and, hence, the degree of membrane perturbation could be mitigated by certain structural modifications of the MIM, in this case fluorination of the central benzene ring of a three-ringed OPV-COE. Additionally, the MIM that perturbed the membrane the least (4,4″-bis(4″-(*N,N*-bis(6″″-(*N,N,N*-trimethylammonium)hexyl)amino)-styryl)stilbene tetraiodide [DSSN+]) was shown in a separate study to have the most electrochemical activity; therefore, it had the greatest potential as a biotechnologically useful modifier (1).

It is reasonable to expect that for MIMs to be useful in a biotechnological context, they must be amenable to use with mixed or environmental cultures; therefore, they must be compatible with a variety of organisms. Despite the recent insights into the effects of OPV-COEs on membranes, these data are limited mainly to *E. coli* K-12 or are based primarily on *in silico* findings with generic Gram-negative model membranes. Using liposomes to mimic mammalian and bacterial membranes, Wang et al. (8) demonstrated the tendency of a similar class of MIMs, phenylene ethynylene oligomer-conjugated COEs (OPE-COEs), to destroy liposomes composed of *E. coli* total lipid extract relative to liposomes composed of mammalian lipids. Hence, they effectively demonstrated that there is a degree of specificity governing the ability of MIMs to disrupt model membranes and that this arises directly from differences in lipid composition. By extension, phylogenetic differences in microbial membrane lipid composition also may lead to undefined and complex interactions between MIMs and the microbial envelope at a taxonomic level. However, the biological relevance of both *in silico* and *in vitro* systems is unclear, as they lack the complexity of microbial cells and may fail to account for how different features of the cellular envelope govern MIM interactions with the microbial cell.

In this contribution, we examine the response of selected Gram-negative and Gram-positive organisms to three OPV-COE MIMs that have been the focus of previous studies (1, 3, 9, 10). Furthermore, using a combination of specific deletion mutants along with a model membrane system, we will explore interactions between OPV-COEs and different components of the cellular envelope. This, to our knowledge, represents the first work exploring the activity of OPV-COE MIMs with multiple microbial genera simultaneously while using membrane deletion mutants and model membranes to explore how this particular class of compounds interacts with the microbial envelope.

## MATERIALS AND METHODS

**Materials.** DSSN+, 1,4-bis(4″-(*N,N*-bis(6″″-(*N,N,N*-trimethylammonium)hexyl)amino)-styryl)benzene tetraiodide (DSBN+), and 1,4-bis(4″-(*N,N*-bis(6″″-(*N,N,N*-trimethylammonium)hexyl)amino)-styryl)-2,3,5,6 tetrafluorobenzene tetraiodide (4F-DSBN+) were syn-

**TABLE 1** Microorganisms and strains used in this study

| Strain | Growth condition(s) | Reference or source |
|---|---|---|
| *E. coli* K-12 | 37°C | ATTC 10798 |
| *E. coli* W3110 | 37°C | *E. coli* Genetic Stock Center, Yale University |
| *E. coli* WBB06 | 37°C, 12 μg/ml tetracycline | 25 |
| *B. megaterium* | 37°C | Laboratory strain |
| *S. oneidensis* MR-1 | 30°C | 50 |
| *Enterococcus faecalis* OG1RF | 37°C | 26 |
| *E. faecalis* OG1RF Δ*mprF1* | 37°C | 26 |
| *E. faecalis* OG1RF Δ*mprF2* | 37°C | 47 |
| *E. faecalis* OG1X Δ*dltA-D* | 37°C | This study |

thesized as reported previously (2, 11). The MIMs used in this study were selected because their biotechnological potential had been demonstrated previously in bioelectrochemical systems and because interesting interactions with microbial cells have been documented (1, 3, 10).

**Organisms and culture conditions.** Unless otherwise stated, all cultures were grown overnight from single colonies in LB medium (244620; Difco, BD, USA) with the exception of *Enterococcus faecalis*, which was grown in brain heart infusion (BHI) medium (256110; Difco, BD, USA). Tetracycline was added at a final concentration of 12 μg ml$^{-1}$ (Table 1). *Escherichia coli* was chosen as a representative Gram-negative organism, and the wild-type laboratory strain (K-12) used in this study was chosen for continuity and compatibility with ongoing work in our laboratory, while W3310 also was used, as this is the parental strain for the deep rough mutant used here (WBB06). *Shewanella oneidensis*, another Gram-negative organism, was chosen because of its electrogenic character and biotechnological relevance to the MIMs under study. A member of the *Bacillus* genus, *B. megaterium*, was selected to represent Gram-positive organisms because its distinctive morphology is experimentally convenient to microscopically distinguish it from other organisms. Finally, *E. faecalis* was chosen because it is a well-studied Gram-positive pathogen that is genetically tractable with known antimicrobial resistance mechanisms and whose coccoid morphology contrasts with the other organisms in this study. An *E. faecalis* Δ*dltA-D* deletion mutant, which is unable to express D-alanylated teichoic acids in its cell wall, allowing for the role of charge-based interactions with the microbial envelope and OPV-COEs to be explored, was constructed as described below. Even though *Staphylococcus aureus dlt* deletion mutants exist, it is preferable to limit mechanistic studies of the Gram-positive envelope to a single species, in this case *E. faecalis*. A summary of the organisms used in this study can be found in Table 1.

**Epifluorescence microscopy.** Images of MIM accumulation in *E. coli* membranes were captured as previously reported (3).

**Construction of *E. faecalis* OG1X Δ*dltA-D* in-frame deletion mutant.** In-frame deletion of *dltA-D* was performed using a plasmid derived from pLT06 (12). Briefly, flanking regions (~1 kb) from both the 5′ and 3′ ends of the *dltABCD* operon were PCR amplified by using the primers indicated. For the construction of the pKS101 plasmid (*dltA-D* deletion), primers DltP1 (5′-GAGAGAATTCTAAGTGGTATGTCTCGTTATG-3′) and DltP2n (5′-CTCTGGATCCCATTATCATTCACCTCCTAAG-3′) were employed to amplify the region 5′ of the translation start site of *dltA* using the available genome sequence from *E. faecalis* V583. Primers DltP3 (5′-GAGAGGATCCTAGTTTCAGAAAGGATGGAATG-3′) and DltP4 (5′-CTCTCTGCAGAGTCAATTTCATGTGTGGACA-3′) were used to amplify the region 3′ of the translation stop site of *dltD*. The DltP1 and DltP2 region contained EcoRI and BamHI sites, and DltP3 and DltP4 contained BamHI and PstI sites. Each product was cut with BamHI, religated, and reamplified with primers DltP1 and DltP4 to obtain an ampli-

**TABLE 2** MICs of DSSN+, DSBN+, and 4F-DSBN+ with a selection of Gram-negative (*E. coli* K-12 and *S. oneidensis* MR1) and Gram-positive (*Enterococcus faecalis* OG1RF and *Bacillus megaterium*) organisms

| | MIC (μM) | | | |
|---|---|---|---|---|
| MIM | *E. coli* K-12 | *S. oneidensis* | *E. faecalis* | *B. megaterium* |
| DSSN+ | 64 | 64 | 8 | 2 |
| 4F-DSBN+ | 4 | 4 | 1 | 1 |
| DSBN+ | 2 | 1 | 1 | 1 |

con deleted for the *dltA-D* genes. This amplicon was digested with EcoRI and PstI and ligated into similarly digested pLT06, and the ligation reaction was desalted and electroporated into electrocompetent *E. coli* ElectroTen-Blue cells (Stratagene, La Jolla, CA). Constructs were screened by colony PCR, and positive clones were further confirmed by restriction mapping and DNA sequencing. The plasmid construct, designated pKS101 and containing the deletion construct for *dltA-D*, was electroporated into electrocompetent *E. faecalis* OG1X cells (13). *E. faecalis* strain OG1XΔdlt was generated by following the protocol previously described (14). Mutants were confirmed by PCR using the primers DltUp (5′-CCT TCTCCAACTACCGCAAC-3′) and DltDown (5′-AATGTCGTACTGCC TGCATC-3′).

**MIC.** MIC tests were carried out using a broth microdilution method as described by Wiegand et al. (15). Briefly, MIMs were diluted in 2-fold dilution series in LB medium to final concentrations ranging from 0.5 μM to 256 μM in a 96-well plate. Each well was inoculated with $5 \times 10^5$ CFU ml$^{-1}$ of the respective organism. Experiments were carried out in triplicate. Growth in each well was monitored spectrophotometrically by measurement of the optical density at 600 nm (OD$_{600}$) over a period of 24 h at 20-min intervals in a Tecan Infinite Pro M200 microplate reader. MIC is defined as the lowest MIM concentration that reduced the growth of bacterial species to <50% of the appropriate control.

**Sample preparation for transmission electron microscopy (TEM).** Overnight cell cultures were pelleted at $10,000 \times g$ for 5 min and suspended in phosphate-buffered saline (PBS) to an OD$_{600}$ of 1. *E. coli* K-12 cells were incubated for 15 min in the dark with 5 and 64 μM DSSN+, 5 μM DSBN+, and 5 μM 4F-DSBN+, while *E. faecalis* cells were treated with 1 μM (each) DSSN+, DSBN, and 4F-DSBN+ in the dark for 15 min. Treatment concentrations were selected to be close to but not above their corresponding MIC values (Table 2), with the exception of DSSN+, where values were selected to correspond to biotechnologically useful concentrations (1) and to be close to the MIC of DSSN+ in *E. coli*, enabling the comparison of the toxic effects of all MIMs in both *E. coli* K-12 and *E. faecalis* using TEM. Following MIM treatment, cells were washed twice with PBS and resuspended to a final OD$_{600}$ of 1.

**Sample processing for transmission electron microscopy.** The bacterial cells were fixed with 7.5 ml of a primary fixative consisting of 1% glutaraldehyde (Agar Scientific, Stansted, United Kingdom) at 4°C for 24 h. After primary fixation, the bacterial cells were washed and postfixed with 1% osmium tetroxide (Ted Pella, Redding, CA, USA) for 2 h. A few grains of potassium ferrocyanide were added to enhance the contrast of the membranous structure within cells. After 2 h, the cell pellets were washed and dehydrated with progressively increasing concentrations of ethanol (25%, 50%, 75%, 95%, and 100%). The dehydration step was enhanced by another two rounds of absolute acetone treatment for 10 min each. Dehydrated cell pellets then were infiltrated with increasing concentrations of araldite 502 (Ted Pella) to acetone at increasing temperatures before being embedded in fresh araldite for 24 h at 60°C. The embedded samples were trimmed with an ultramicrotome (Reichert-Jung, Depew, NY, USA) to approximately 50 to 70 nm. Cut sections then were placed onto a 200-mesh copper grid before being stained with 2% uranyl acetate and postfixed with lead citrate. Stained sections were viewed using a JEOL 1010 transmission electron microscope and captured digitally with a dual-view digital camera (Gatan Inc., Werrendale, CA, USA).

**Confocal laser scanning microscopy.** Eight-chamber slides (product no. 80801; ibidi, Germany) were pretreated with poly-L-lysine. *E. coli* K-12 and *B. megaterium* cells were grown overnight in LB medium and diluted in 1 ml PBS to a final OD$_{600}$ of 1 and 0.15, respectively. One hundred microliters of the mixture was added to each chamber and left to settle for an hour. Cells next were washed twice with PBS. Twenty μl of fresh PBS was left in each chamber, to which 20 μl of 2 μM DSSN+ was added. The time-lapse uptake of DSSN+ by a mixed culture was visualized with a confocal microscope (LSM-780; Carl Zeiss, Germany) using an excitation wavelength of 405 nm and an emission window set from 415 to 700 nm.

**Solvatochromic changes in response to phospholipids.** Liposomes were prepared using thin-film hydration and extrusion from commercially available *E. coli* total lipid extracts and *E. coli* extracts of phosphatidylglycerol (PG), phosphatidylethanolamine (PE), and diphosphatidylglycerol (DPG) (Avanti Polar Lipids, Inc., USA) with increasing amounts of DPG from 10% (wt/vol) to 33% (wt/vol). Briefly, 50 mM lipids was dissolved in chloroform in a round-bottom flask and dried under a constant stream of nitrogen gas. The resulting film was suspended in HEPES buffer and vortexed to a homogenous suspension. An extruder was heated and maintained at 55°C. After this step, the suspension was passed through 400-nm and 100-nm polycarbonate filters sequentially to obtain small unilamellar liposomes. Liposomes were kept at 4°C until use. Liposomes were suspended in PBS (pH ≈7.4), treated with 5 μM each MIM (DSSN+, DSBN+, and 4F-DSBN+), and subjected to an emission scan at the corresponding absorbance maximum for each MIM (414 to 427, 406 to 428, and 430 to 436 nm for DSSN+, DSBN+, and 4F-DSBN+, respectively). The Stoke's shift was calculated as the difference between the absorbance and emission maximum and compared with that observed for each MIM in PBS buffer alone. Optical experiments were performed in 96-well plates using a Tecan Infinite Pro M200 microplate reader in absorbance and emission scan mode at 2-nm intervals. To rule out concentration-dependent solvatochromic effects, experiments were repeated with 2.5 and 10 μM concentrations of each MIM.

## RESULTS AND DISCUSSION

The three MIMs used in this study (DSSN+, DSBN+, and 4F-DSBN+; Fig. 1 depicts molecular structures) spontaneously associate with the microbial envelope. This is evident from the representative micrograph of *E. coli* cells stained with 5 μM DSSN+ (Fig. 2) and consistent with previous reports (2, 3). All three MIMS are thought to reside in the microbial membrane based on well-documented observations of their optical characteristics, which are manifested as blue-shifted emission maxima following association with the membrane compared with the emission maxima in water, along with an increase in quantum yield as evidenced from the high contrast in the micrographs (Fig. 2) (2, 3, 10). The fluorescent signal from DSSN+ can be tracked in treated *E. coli* daughter cells for over 30 divisions (Fig. 2), suggesting not only the strong interactions between the MIM and the microbial envelope but also that the viability of *E. coli* is not compromised by treatment with 5 μM DSSN+. This points to a stable configuration of DSSN+ in biological membranes and the potential to modify membrane properties over extended periods.

**Toxicity.** For DSSN+, the most well-tolerated MIM, the MIC for both *E. coli* and *Shewanella oneidensis* was 64 μM, and for *E. faecalis* and *B. megaterium* it was 8 and 2 μM, respectively (Table 2). DSBN+ and 4F-DSBN+ are similarly toxic. The toxicity profiles for *E. coli* K-12, the only organism for which OPV-COE toxicity data exist, are in agreement with other reports (1, 3). The DSSN+ MIC for *E. coli* and *S. oneidensis* (64 μM is approximately 100 mg liter$^{-1}$) is not particularly high compared to antimicrobial MIMs, some of which can be active at concentrations in the μg
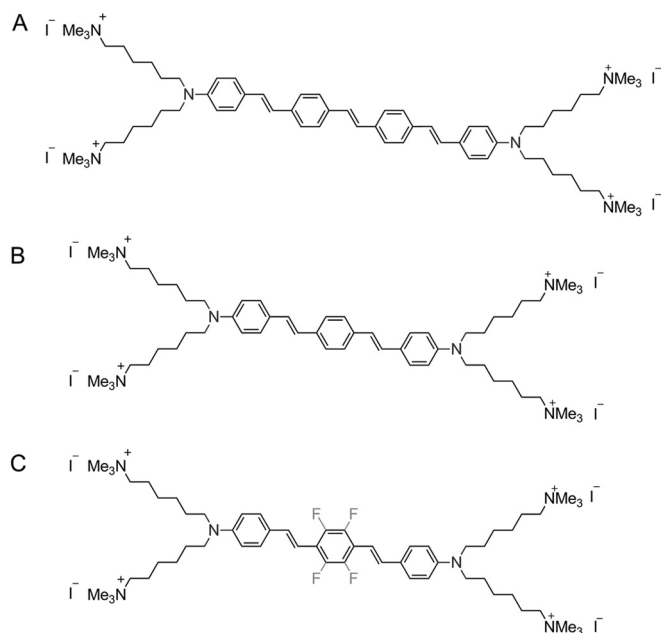
Hinks et al.



FIG 1 Molecular diagram representing the MIMs in this study: DSSN+ (A), DSBN+ (B), and 4F-DSBN+ (C). Adapted with permission from reference 3 (copyright 2014, American Chemical Society).

liter$^{-1}$ range, and is roughly double that of magainin (16–18). Conversely, the toxicity of DSBN+ and 4F-DSBN+ for all organisms and, in particular, Gram-positive organisms (MIC for *E. faecalis*, ≈3 to 6 mg liter$^{-1}$) is such that these compounds can be considered to have antimicrobial activity that is approaching a clinically interesting range and which is comparable with nisin and traditional β-lactams, like penicillin and imipenem (16, 17). Aside from the differences in the toxicity profile based on the molecular characteristics, there is a difference in MIM toxicity that is determined by an organism's Gram status. *E. faecalis* and *B. megaterium*, both of which are Gram-positive organisms, are relatively more susceptible to MIMs than the Gram-negative organisms tested here. This is evident by MICs of 1 μM for all OPV-

COEs, with the exception of DSSN+ for both *E. faecalis* and *B. megaterium*. The preferential ability of small molecules to disrupt Gram-positive membranes is well documented, and many amphiphilic, cationic peptides, such as the bacteriocins derived from lactobacilli as well as glycopeptides like vancomycin, have an antimicrobial specificity for Gram-positive organisms (19).

**Evidence of membrane damage.** TEM images of *E. faecalis* incubated with 1 μM DSSN+, DSBN+, or 4F-DSBN+ (Fig. 3) show extensive membrane damage relative to similar incubations with *E. coli* (Fig. 4), even though the latter were treated with higher MIM concentrations (5 and 64 μM). The TEM data support the toxicity profiles (Table 2) indicating that Gram-positive organisms are more sensitive to MIMs than Gram-negative organisms. The primary toxic event following MIM treatment is likely the disruption of biological membranes, and this is true for both Gram-positive and Gram-negative organisms, albeit at relatively higher concentrations for the latter. In addition to differences in the absolute MIM susceptibility between Gram types, the mechanism of membrane perturbation appears to be different; Gram-negative *E. coli* appeared ruptured at the end caps, possibly as a result of osmotic swelling, whereas the cell membrane of the Gram-positive *E. faecalis* appeared extensively porated and discontinuous in comparison (Fig. 3 and 4). However, morphological changes in response to general cytotoxicity, including the effects of the membrane-disrupting antimicrobial peptide nisin on *E. faecalis* (20), are well documented and may explain these observations (21).

**Role of OM.** There are obvious differences in the cell envelopes of Gram-positive and Gram-negative organisms, and these differences could explain their differential sensitivity to MIMs. Gram-negative organisms have both an outer membrane (OM) and an inner, cytoplasmic membrane separated by a thin, moderately cross-linked peptidoglycan layer. Additionally, the outer membrane of Gram-negative organisms incorporates a negatively charged lipopolysaccharide (LPS) layer that acts as a molecular sieve, impeding the passage of small molecules across the cellular envelope. The protective effect of the Gram-negative OM to certain antibiotics is well documented (17, 22–24).

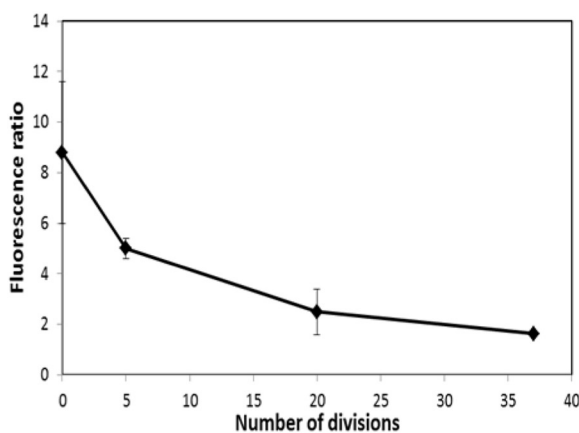The tight packing of the six fatty acid components of lipid A of



FIG 2 Mean fluorescence foreground-to-background ratio ($n = 9$; error bars show relative standard deviations) of *E. coli* treated with 5 μM DSSN+ over time, along with an epifluorescence micrograph of *E. coli* treated with 10 μM DSSN+ after approximately five divisions. The micrograph shows the association of DSSN+ with the membrane. The optical properties are consistent with the MIM being in a nonpolar milieu. Uptake images and optical spectra on association with microbial membranes for all of the MIMs used in this study have been reported elsewhere (34).
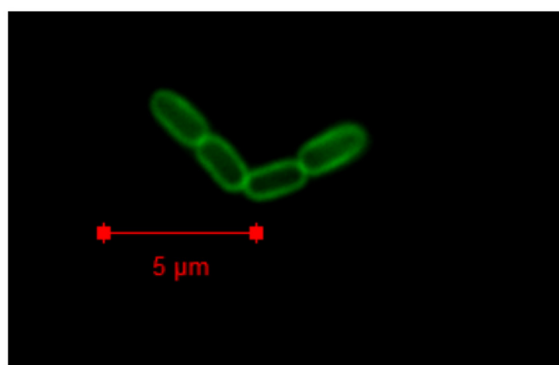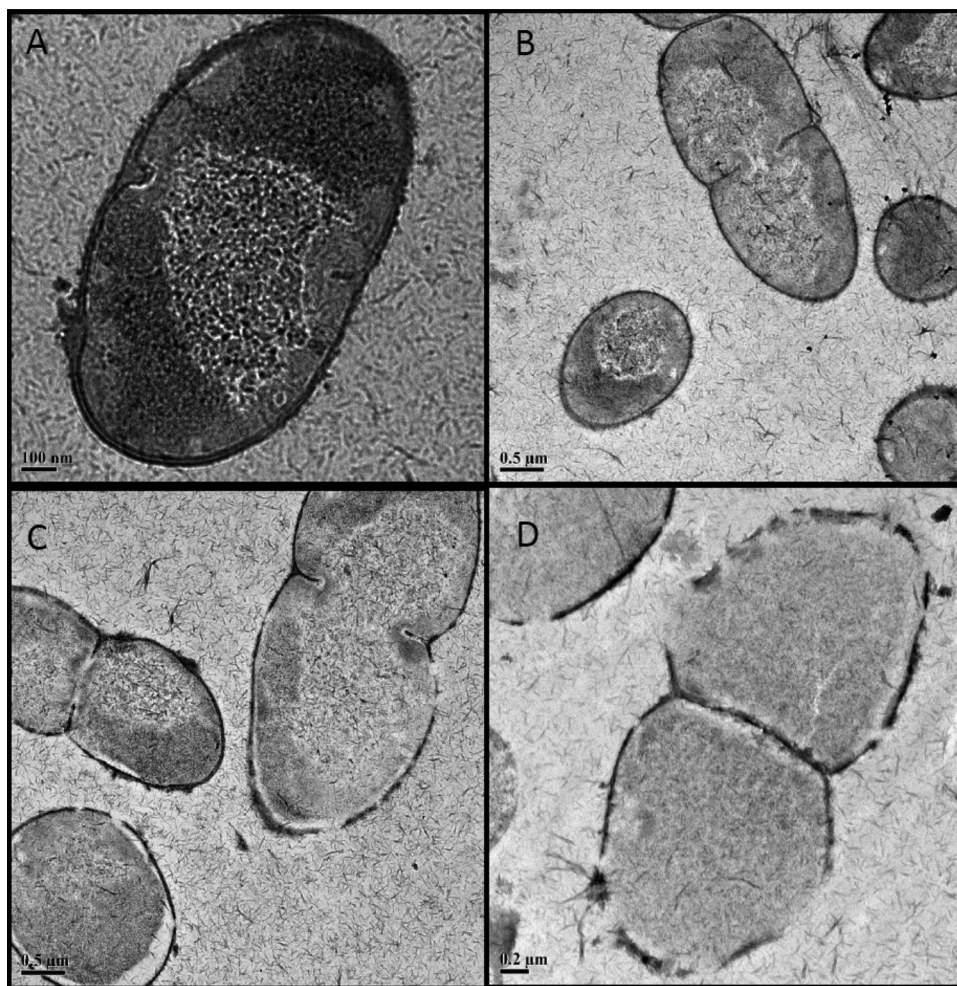
**FIG 3** Micrographs (TEM) of *E. faecalis* (A) treated with 1 μM DSSN+ (B), DSBN+ (C), and 4F-DSBN+ (D). Note the discontinuous membranes in the treated cells, in particular those treated with DSBN+ and 4F-DSBN+, despite the low concentration of MIMs relative to *E. coli* treatments (5 μM and 64 μM for DSSN+ and 5 μM for both DSBN+ and 4F-DSBN+; see Fig. 4). This micrograph shows that membrane disruption is a key mode of action for these compounds and that Gram-positive membranes are more extensively damaged by MIM insertion than are those from Gram-negative organisms. These observations are supported by the MIC tests (Table 2).

the LPS layer is thought to underlie the impervious nature of the Gram-negative OM (23, 24). A range of *E. coli* mutants, which have profound defects in the lipid A component of the LPS in the OM, have a phenotype that is described as deep rough. These mutants usually are immobile and susceptible to a number of antimicrobials (22). It is the lack of a continuous LPS layer that underlies the increased susceptibility of deep rough strains to certain antimicrobials. Accordingly, deep rough mutants have been proposed as useful tools for studying the interactions between antimicrobials and their target organisms (22, 23, 25). *E. coli* WBB06 is a mutant deficient in heptosyltransferase I (*rfaC*) and II (*rfaF*), which expresses a truncated lipid A inner core and has a typical deep rough phenotype (22). WBB06 did not differ in sensitivity to DSSN+, DSBN+, or 4F-DSBN+ from its parental strain, *E. coli* W3110 (Table 3), suggesting that the LPS layer is not the main protective element in differentiating Gram-negative and Gram-positive susceptibility to the MIMs used in this study. While molecules of <600 Da can easily pass through the LPS layer, the molecules tested here are in the range of 1,389 to 1,491 Da;

therefore, the linear topology of the OPV-COEs likely explains the ease with which they can penetrate the LPS layer (25).

**Role of surface charge.** In a mixed culture of *E. coli* and *B. megaterium* treated with 5 μM DSSN+, the larger (>10 μM) Gram-positive *B. megaterium* preferentially accumulated DSSN+ (Fig. 5), suggesting that the cell wall did not significantly hinder the uptake of this MIM. Gram-positive organisms lack an outer membrane and have a characteristically thick and highly cross-linked peptidoglycan layer and only a single cytoplasmic membrane. In contrast to Gram-negative organisms, the negative charge of the Gram-positive cell envelope results predominantly from teichoic acid and anionic phospholipids. The anionic nature of certain phospholipids is thought to govern the interaction between microbes and some cationic antimicrobial peptides (26). Therefore, it is possible that the charged components, or rather the distribution of charge, throughout the Gram-positive envelope drives the preferential uptake and the susceptibility of Gram-positive organisms to the MIMs used in this study.
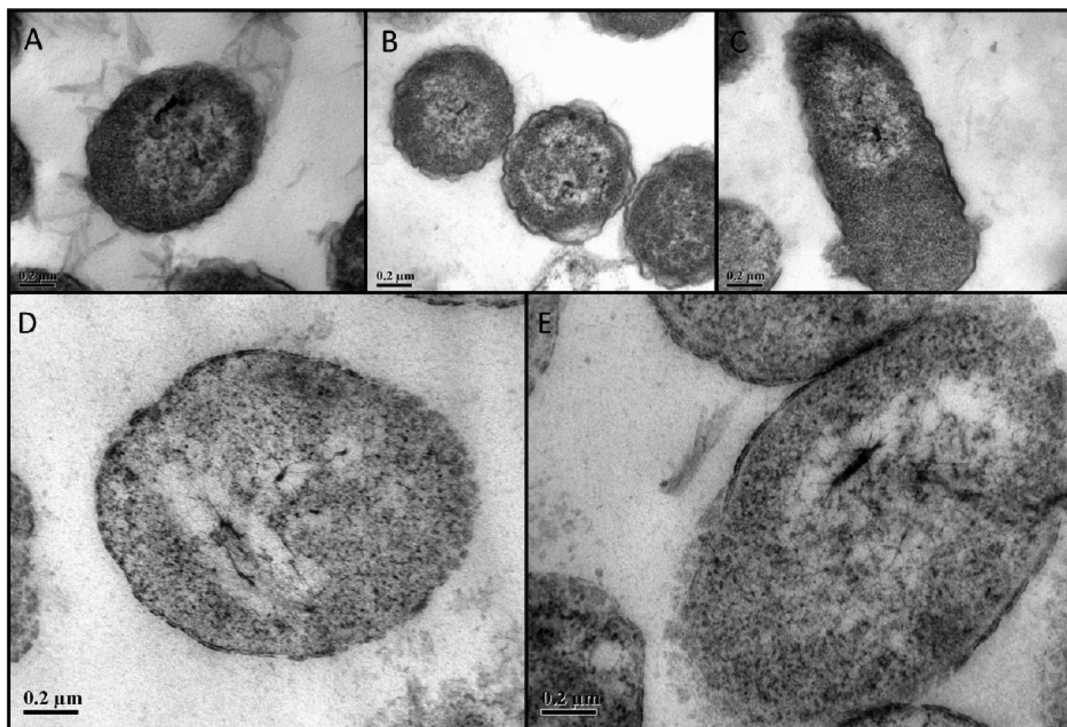
**FIG 4** Micrographs (TEM) of *E. coli* (A) treated with 5 µM (B) and 64 µM DSSN+ (C), 5 µM DSBN+ (D), and 5 µM 4F-DSBN+ (E). The micrographs support the MIC data (Table 2) demonstrating membrane damage by DSBN+ (C) and 4F-DSBN+ (D) at lower concentrations (5 µM) than those of DSSN+, where membrane damage is apparent only in cells treated with 64 µM DSSN+ (C). The cell membranes appear ruptured at the end caps, an eventuality which could result from osmotic swelling.

**Aminoacylated phospholipids.** Altering the surface charge of the microbial envelope, in particular the cytoplasmic membrane, is a well-known mechanism whereby organisms can elaborate resistance to certain antimicrobials by diminishing the magnitude of charge-based interactions (26, 27). The multiple peptide resistance factor (*mprF*) virulence factors in *Staphylococcus aureus* and *Enterococcus faecalis* modulate the aminoacylation of the lipid phosphatidylglycerol (PG) to lysylphosphatidylglycerol (L-PG) and a number of other aminophosphatidylglycerols (26). The addition of the cationic L-lysine to the head group of the anionic lipid PG by *mprF* causes the net surface charge of the cytoplasmic membrane to become more positive, which repels certain cationic peptides, such as the human β-defensins, and confers resistance to a number of antimicrobial compounds which target the cellular membrane of Gram-positive organisms (26, 28, 29). There are two known paralogs of *mprF* in *E. faecalis*, *mprF1* and *mprF2*. *mprF2* appears to be more important in mediating the aminoacylation of PG than *mprF1*; hence, *mprF2* deletion mutants are more susceptible to human β-defensins (26–29).

In this study, *mprF1* and *mprF2* deletion mutants of *E. faecalis* OG1RF were not differentially susceptible to either DSSN+, DSBN+, or 4F-DSBN+; therefore, the mechanistic interaction of these compounds with Gram-positive cellular membranes is different from the electrostatic interactions that characterize how cationic peptides such as β-defensins interact with these organisms. Furthermore, the interaction between OPV-COE MIMs and the microbial membrane is not likely to be mediated by PG, as curtailing the organism's ability to alter its properties, i.e., the charge of the normally anionic lipid by aminoacylation, does not change the MIC of these compounds. L-PG expression by *E. faecalis* has been documented under growth conditions identical to those used in this study, as has the lack of resistance to human β-defensins in Δ*mprF* strains through their inability to aminoacy-

**TABLE 3** MICs of DSSN+, DSBN+, and 4F-DSBN+ for a number of mutant strains with defective or missing cellular envelope components known to govern interactions with certain antimicrobial compounds

| Cellular component, parameter, or strain[a] | MIC (µM) | | |
|---|---|---|---|
| | DSSN+ | DSBN+ | 4F-DSBN+ |
| LPS | | | |
| *E. coli* W3110 (parental strain) | 128 | 1 | 1 |
| *E coli* WBB06 Δ*rfaC* Δ*rfaF* | 128 | 1 | 0.5 |
| | | | |
| Charge | | | |
| *E. faecalis* OG1RF Δ*mprF1* | 8 | 1 | 1 |
| *E. faecalis* OG1RF Δ*mprF2* | 8 | 1 | 1 |
| *E. faecalis* OG1X (parental strain) | 8 | 1 | 1 |
| *E. faecalis* OG1X Δ*dltA-D* | 8 | 1 | 0.5 |
| | | | |
| Lipid II | | | |
| *E. faecalis* V583 | 4 | 1 | 0.5 |

[a] *E. coli* WBB06 is a deep rough strain with a defective lipid A core caused by the deletion of genes encoding heptosyl transferase I (*rfaC*) and II (*rfaF*) and its parental wild type (*E. coli* W3110). *E. faecalis* OG1RF Δ*mprF1* and OG1RF Δ*mprF2* have limited ability to aminoacylate phosphatidylglycerol; thus, the extent to which they can modify the net charge of the cytoplasmic membrane is diminished. *E. faecalis* OG1X Δ*dltA* cannot modify the D-alanation of teichoic acids; therefore, it has a limited ability to modify cell wall charge. The vancomycin-resistant *E. faecalis* V583 has a modification in the pentapeptide chain of lipid II, affecting interactions between small molecules and the microbial envelope.
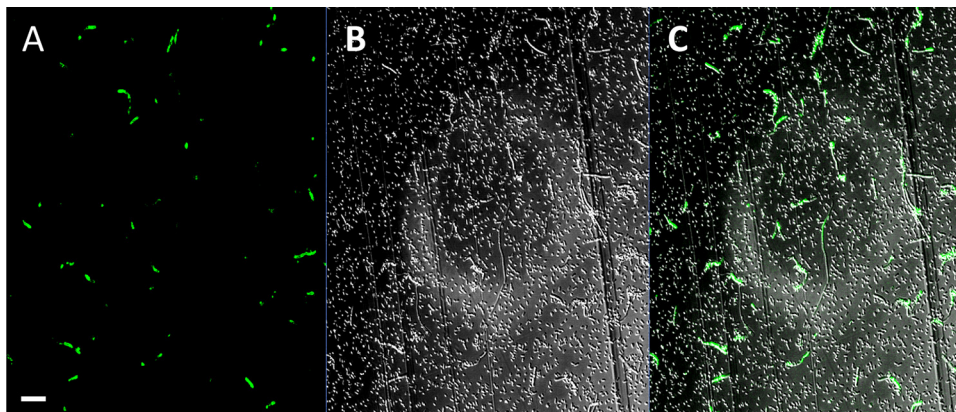
**FIG 5** Confocal laser scanning microscopy micrograph of a binary culture of *E. coli* and *B. megaterium* treated with 5 μM DSSN+. (A) Fluorescence channel; (B) bright-field image; (C) overlay. The large (>5-μm) *B. megaterium* cells have preferentially accumulated the DSSN+ compared to the smaller (≈2-μm) *E. coli* cells. The observation shows an affinity of DSSN+ for Gram-positive organisms and that the peptidoglycan cell wall does not hinder the passage of the MIMs into the cell membrane. Bar, 5 μm.

late PG (26). Because of this and the lack of a phenotype for all of the compounds tested in this study, confirmation of L-PG expression was deemed unnecessary and was not undertaken.

**Teichoic acids.** An additional charge modification of the Gram-positive microbial envelope is conferred by the *dlt* operon that mediates the D-alanylation of lipoteichoic acids in the Gram-positive cell wall (30–32). Like the aminoacylation of PG, the incorporation of D-alanine into the cell wall confers resistance to a number of antimicrobial peptides, including nisin, polymyxin B, and colistin (26, 32, 33). The MICs of the *dltA-D* deletion mutant of *E. faecalis* OG1X were almost identical to those of the wild type (4, 1, and 0.5 μM for DSSN+, DSBN+, and 4F DSBN+, respectively; Table 3). The inability to resist both colistin and nisin has been demonstrated in Δ*dltA* mutants of *E. faecalis* 1230 in rich medium under growth conditions almost identical to those used in this study, and the absence of D-alanine was shown by nuclear magnetic resonance. The lack of a phenotype being observed for either DSSN+, DSBN+, or 4F-DSBN+ with the Δ*dltA* mutant indicates that the role of surface charge in OPV-COE membrane interactions is minor.

**Hydrophobic interactions.** Although both PG and DPG are anionic, the increased susceptibility of Gram-positive organisms, which contain a large amount of DPG in their cellular envelope, compared to that of Gram-negative organisms to OPV-COEs is not likely to be governed by charge-based interactions, as shown by the study with *mprF* and *dlt* deletion mutants of *E. faecalis*. Additionally, for DPG-mediated membrane disruption, it has been shown that the interaction is more complex than the molecules simply having opposing charges (34). Taken together, the evidence with *E. faecalis* Δ*mprF* and Δ*dltA* (Table 3) mutants, along with the preferential uptake of OPV-COE MIMs by a Gram-positive organism, *B. megaterium*, relative to *E. coli* suggests that the interactions between DSSN+, DSBN+, and 4F-DBSN+ and the cellular envelope are of a hydrophobic nature rather than an electrostatic one (30, 33).

**Role of phospholipids.** The main phospholipids in microbial cell membranes are PG and PE. The anionic lipid DPG is a minor component (<5%) of Gram-negative membranes but a major component of Gram-positive membranes (35–38). It is reasonable to assume that the main effects underlying the interactions

between MIMs and the cytoplasmic membrane are driven by major membrane components. The role of PG in mediating the interaction between the MIMs is not likely to be of a significant magnitude, as there was no difference in the sensitivity to OPV-COEs of *E. faecalis mprF* mutants, which express L-PG. In this aspect, it is likely that a specific interaction between DPG and OPV-COEs exists, as DPG is a major component of Gram-positive cellular membranes.

The optical properties of DSSN+, DSBN+, and 4F-DSBN+ are dependent upon the polarity of their environment, and both the absorbance and emission characteristics change in response to solvation state and concentration, the latter being driven by the extent of aggregation (38, 39). The solvatochromic response to decreasing solvent polarity for OPV-COEs is negative; hence, it is manifest as a blue-shifted emission spectrum which can also be expressed as a decrease in the Stoke's shift relative to emission spectra in water. The solvatochromic behavior of OPV-COEs has been used successfully to confirm the uptake of these MIMs into microbial membranes and also their perpendicular arrangement to the bilayer plane in vesicles composed of mammalian lipids (40). The optical characteristics of lipid soluble chromophores (e.g., Laurdan) are used routinely to assess membrane characteristics, such as lipid order, that are indicative of bilayer perturbation in model and *in vivo* systems (41).

In large unilamellar vesicles (LUVs) prepared from *E. coli* total lipid extract and treated with DSSN+, DSBN+, and 4F-DSBN+, there was a marked negative solvatochromic effect, manifest as a smaller Stoke's shift (84 to 88 nm) compared with that determined with OPV-COEs in polar buffer alone (131 to 170 nm) (Table 4). The negative solvatochromic effect, indicative of tight membrane packing, was largely conserved in LUVs prepared from 9:1 PE:PG, with Stoke's shifts ranging from 71 to 86 nm (Table 4). However, in LUVs containing a large proportion of DPG (1:1:1 PE:PG:DPG), the negative solvatochromic effect was diminished for all MIMS, with the exception of DSBN+, which remained largely unchanged in response to lipid content. The Stoke's shift was 118, 84, and 94 nm for DSSN+, 4F-DSBN+, and DSBN+, respectively (Table 4). An increase in Stoke's shift can be interpreted as being indicative of an increase in solvent polarity of the OPV-COE medium, which is consistent with membrane damage either from the

**TABLE 4** Stoke's shifts of MIMs in liposomes composed of *E. coli* extract, a generic Gram-negative model membrane, and a Gram-positive model membrane

| MIM | Stoke's shift (nm) | | | |
|-----|-------|---------------|-----------|-------------------|
| | HEPES | *E. coli* extract | PE:PG (9:1) | PE:PG:DPG (1:1:1) |
| DSSN+ | 170 | 84 | 88 | 118 |
| 4F-DSBN+ | 144 | 88 | 71 | 94 |
| DSBN+ | 131 | 86 | 91 | 84 |

formation of pores or water channels, disordering of the acyl chains, or destruction of the membrane bilayer. Taken together with the MIC tests (Table 2) and the micrographic evidence of membrane damage (Fig. 3 and 4), the data presented here suggest there are lipid-based drivers governing the interactions between OPV-COEs and the microbial envelope which underlie the differential sensitivity of Gram-negative and Gram-positive organisms to these compounds.

**Mechanisms.** Nisin is an amphiphilic broad-spectrum cationic antimicrobial peptide produced by *Streptococcus lactis* that is active against Gram-positive bacteria and which has been widely used in the food industry since the 1960s (2). Microbes that have acquired resistance to nisin have bulk changes in their membrane phospholipid head group composition and have been shown to contain less DPG than their wild-type counterparts. Furthermore, the importance of DPG content in antimicrobial susceptibility has been demonstrated using model membrane systems (20, 42–45). Additionally, apoptosis in mitochondria has been shown to be inextricably linked to DPG and its affinity for cytochrome *c*, with the DPG content increasing from ≈4% to in excess of 20% immediately prior to apoptosis (45–47). Therefore, the increased content of DPG in Gram-positive microbial membranes likely underlies the sensitivity of Gram-positive organisms to OPV-COEs.

Nisin interacts with the lipid precursor, lipid II, and can have up to a 700-fold increase in activity against active cells compared to protoplasts, an observation attributed to a general low-affinity permeability interaction with DPG and a targeted lipid II-dependent poration mechanism (46, 47). It is unlikely that a similar lipid II-dependent mechanism exists with OPV-COEs, as it is an interaction driven by a specificity with the D-Ala-D-Ala pentapeptide chain that stabilizes the lipid II molecule, and no such specific binding site exists on OPV-COEs. Furthermore, the MICs (8, 1, and 0.5 μM for DSSN+, DSBN+, and 4F-DSBN+, respectively) of vancomycin-resistant strains of *E. faecalis* (VRE V583; Table 3), an organism whose antimicrobial resistance properties are conferred via mutations in pentapeptide of lipid II, were almost identical to those of nonresistant strains (16).

The exceptionally large (>1) critical packing parameter of double-headed DPG makes it prone to disruption by MIM insertion (16, 19, 34). DPG has a conical cross section, because the acyl chains have a larger cross-sectional area than the phosphate head group. The thermodynamics of this geometry is disrupted by MIMs to a greater extent than it is for lipids which have a smaller critical packing parameter (<1) than DPG and a more accommodating cylindrical or inverted cone cross section that has less energetic resistance to tighter packing (48). Kumar has shown that the lipid lamellar phase is maintained only at a critical packing parameter of around 0.74 and that deviations from this can desta-

bilize membranes (49). Furthermore, the larger size of DPG means that there will be fewer intramolecular spaces for MIMs to occupy, and local concentrations of MIM may be higher in the intermolecular spaces of DPG for a given surface area than for single-head phospholipids. In short, the geometry of DPG causes it to have a preference for negative curvature, and when it exists in a planar bilayer, it is more prone to undergo conformational changes in response to perturbations, an assertion which is supported by the solvatochromic effects observed with model membranes (Table 4) (38, 47–49).

This study points toward a specific DPG-destabilizing effect of MIMs, a finding that has a clear explanation and precedence, both in the membrane-perturbing mechanism of nisin and in mitochondrial apoptosis. The MIMs used in this study perturb membranes via a hydrophobic mismatch between the length of the lipid acyl chains and the length of the MIM (3, 7). Therefore, it is likely that in addition to the interaction with DPG, there also exists molecular-scale interaction between the acyl chains, further bolstering the idea of a predominantly hydrophobic interaction of this class of compounds. Because OPV-COE activity is driven mainly by a hydrophobic interaction with lipids, they are ideal compounds to study with simple model systems, including molecular dynamics simulations. Therefore, with a specially selected mutant library (that must include mutants deficient in lipin synthases), a powerful platform to assess membrane interactions could be developed that will allow the informed development of biotechnologically useful MIMs. Focusing on the membrane does not rule out secondary toxic mechanisms, and future studies need to ascertain the role of secondary targets in MIM sensitivity. It is essential that future studies include a variety of organisms, including anaerobes, to assess the generality of the findings in this paper. Finally, future work should not ignore the antimicrobial properties of DSBN+ and 4F-DSBN+ or the interesting observation that they circumvent common resistance mechanisms in *E. faecalis* (i.e., *mprF*, *dlt*, and lipid II). Previous studies have offered evidence for the modification of microbial membranes using a certain class of MIMs, OPV-COEs. This study is, to our knowledge, the first to investigate the compatibility of this emerging class of compounds with a number of microbes. We have shown that the proposed use of MIMs to modify the properties of microbial membranes is feasible, because a stable configuration of at least one MIM (DSSN+) in microbial membranes is possible. However, OPV-COEs are inhibitory to Gram-positive microbes, and TEM analysis has shown the likely mechanism lies in their tendency to damage cell membranes. Therefore, the current format of the MIMs used in this study is not compatible with Gram-positive organisms, and designing compounds for this purpose represents a research opportunity.

## REFERENCES

1. **Wang VB, Du J, Chen X, Thomas AW, Kirchhofer ND, Garner LE, Maw MT, Poh WH, Hinks J, Wuertz S, Kjelleberg S, Zhang Q, Loo JS, Bazan GC.** 2013. Improving charge collection in Escherichia coli-carbon electrode devices with conjugated oligoelectrolytes. Phys Chem Chem Phys **15:**5867–5872. http://dx.doi.org/10.1039/c3cp50437a.
2. **Garner LE, Park J, Dyar SM, Chworos A, Sumner JJ, Bazan GC.** 2010. Modification of the optoelectronic properties of membranes via insertion of amphiphilic phenylenevinylene oligoelectrolytes. J Am Chem Soc **132:**10042–10052. http://dx.doi.org/10.1021/ja1016156.
3. **Hinks J, Wang Y, Poh WH, Donose BC, Thomas AW, Wuertz S, Loo SCJ, Bazan GC, Kjelleberg S, Mu Y, Seviour T.** 2014. Modeling cell membrane perturbation by molecules designed for transmembrane electron transfer. Langmuir **30:**2429–2440. http://dx.doi.org/10.1021/la403409t.
4. **Bradshaw J.** 2003. Cationic antimicrobial peptides. BioDrugs **17:**233–240. http://dx.doi.org/10.2165/00063030-200317040-00002.
5. **Last NB, Miranker AD.** 2013. Common mechanism unites membrane poration by amyloid and antimicrobial peptides. Proc Natl Acad Sci U S A **110:**6382–6387. http://dx.doi.org/10.1073/pnas.1219059110.
6. **Seo M-D, Won H-S, Kim J-H, Mishig-Ochir T, Lee B-J.** 2012. Antimicrobial peptides for therapeutic applications: a review. Molecules **17:**12276–12286. http://dx.doi.org/10.3390/molecules171012276.
7. **Strandberg E, Esteban-Martín S, Ulrich AS, Salgado J.** 2012. Hydrophobic mismatch of mobile transmembrane helices: merging theory and experiments. Biochim Biophys Acta **1818:**1242–1249. http://dx.doi.org/10.1016/j.bbamem.2012.01.023.
8. **Wang Y, Tang Y, Zhou Z, Ji E, Lopez GP, Chi EY, Schanze KS, Whitten DG.** 2010. Membrane perturbation activity of cationic phenylene ethynylene oligomers and polymers: selectivity against model bacterial and mammalian membranes. Langmuir **26:**12509–12514. http://dx.doi.org/10.1021/la102269y.
9. **Du J, Thomas AW, Chen X, Garner LE, Vandenberg CA, Bazan GC.** 2013. Increased ion conductance across mammalian membranes modified with conjugated oligoelectrolytes. Chem Commun **49:**9624–9626. http://dx.doi.org/10.1039/c3cc45094e.
10. **Hou H, Chen X, Thomas AW, Catania C, Kirchhofer ND, Garner LE, Han A, Bazan GC.** 2013. Conjugated oligoelectrolytes increase power generation in E. coli microbial fuel cells. Adv Mater **25:**1593–1597. http://dx.doi.org/10.1002/adma.201204271.
11. **Woo HY, Liu B, Kohler B, Korystov D, Mikhailovsky A, Bazan GC.** 2005. Solvent effects on the two-photon absorption of distyrylbenzene chromophores. J Am Chem Soc **127:**14721–14729. http://dx.doi.org/10.1021/ja052906g.
12. **Thurlow LR, Thomas VC, Hancock LE.** 2009. Capsular polysaccharide production in Enterococcus faecalis and contribution of CpsF to capsule serospecificity. J Bacteriol **191:**6203–6210. http://dx.doi.org/10.1128/JB.00592-09.
13. **Shepard BD, Gilmore MS.** 1995. Electroporation and efficient transformation of Enterococcus faecalis grown in high concentrations of glycine. Methods Mol Biol **47:**217–226.
14. **Kristich CJ, Chandler JR, Dunny GM.** 2007. Development of a host-genotype-independent counterselectable marker and a high-frequency conjugative delivery system and their use in genetic analysis of Enterococcus faecalis. Plasmid **57:**131–144. http://dx.doi.org/10.1016/j.plasmid.2006.08.003.
15. **Wiegand I, Hilpert K, Hancock REW.** 2008. Agar and broth dilution methods to determine the minimal inhibitory concentration (MIC) of antimicrobial substances. Nat Protoc **3:**163–175. http://dx.doi.org/10.1038/nprot.2007.521.
16. **Breukink E, de Kruijff B.** 2006. Lipid II as a target for antibiotics. Nat Rev Drug Discov **5:**321–323. http://dx.doi.org/10.1038/nrd2004.
17. **Tong Z, Zhang Y, Ling J, Ma J, Huang L, Zhang L.** 2014. An in vitro study on the effects of nisin on the antibacterial activities of 18 antibiotics against Enterococcus faecalis. PLoS One **9:**e89209. http://dx.doi.org/10.1371/journal.pone.0089209.
18. **Maria-Neto S, Cândido EDS, Rodrigues DR, de Sousa DA, da Silva EM,** de Moraes LMP, Otero-Gonzalez ADJ, Magalhães BS, Dias SC, Franco OL. 2012. Deciphering the magainin resistance process of Escherichia coli strains in light of the cytosolic proteome. Antimicrob Agents Chemother **56:**1714–1724. http://dx.doi.org/10.1128/AAC.05558-11.
19. **Ennahar S, Sonomoto K, Ishizaki A.** 1999. Class IIa bacteriocins from lactic acid bacteria: antibacterial activity and food preservation. J Biosci Bioeng **87:**705–716. http://dx.doi.org/10.1016/S1389-1723(99)80142-X.
20. **Ruhr E, Sahl H-G.** 1985. Mode of action of the peptide antibiotic nisin and influence on the membrane potential of whole cells and on cytoplasmic and artificial membrane vesicles. Antimicrob Agents Chemother **27:**841–845. http://dx.doi.org/10.1128/AAC.27.5.841.
21. **Nonejuie P, Burkart M, Pogliano K, Pogliano J.** 2013. Bacterial cytological profiling rapidly identifies the cellular pathways targeted by antibacterial molecules. Proc Natl Acad Sci U S A **110:**16169–16174. http://dx.doi.org/10.1073/pnas.1311066110.
22. **Vaara M, Nurminen M.** 1999. Outer membrane permeability barrier in Escherichia coli mutants that are defective in the late acyltransferases of lipid A biosynthesis. Antimicrob Agents Chemother **43:**1459–1462.
23. **Raetz CRH, Garrett TA, Reynolds CM, Shaw WA, Moore JD, Smith DC, Ribeiro AA, Murphy RC, Ulevitch RJ, Fearns C, Reichart D, Glass CK, Benner C, Subramaniam S, Harkewicz R, Bowers-Gentry RC, Buczynski MW, Cooper JA, Deems RA, Dennis EA.** 2006. Kdo2-lipid A of Escherichia coli, a defined endotoxin that activates macrophages via TLR-4. J Lipid Res **47:**1097–1111. http://dx.doi.org/10.1194/jlr.M600027-JLR200.
24. **Mohanram H, Bhattacharjya S.** 2014. Resurrecting inactive antimicrobial peptides from lipopolysaccharide trap. Antimicrob Agents Chemother **58:**1987–1996. http://dx.doi.org/10.1128/AAC.02321-13.
25. **Brabetz W, Muller-Loennies S, Holst O, Brade H.** 1997. Deletion of the heptosyltransferase genes rfaC and rfaF in Escherichia coli K-12 results in an Re-type lipopolysaccharide with a high degree of 2-aminoethanol phosphate substitution. Eur J Biochem **247:**716–724. http://dx.doi.org/10.1111/j.1432-1033.1997.00716.x.
26. **Kandaswamy K, Liew TH, Wang CY, Huston-Warren E, Meyer-Hoffert U, Hultenby K, Schröder JM, Caparon MG, Normark S, Henriques-Normark B, Hultgren SJ, Kline KA.** 2013. Focal targeting by human β-defensin 2 disrupts localized virulence factor assembly sites in Enterococcus faecalis. Proc Natl Acad Sci U S A **110:**20230–20235. http://dx.doi.org/10.1073/pnas.1319066110.
27. **Sohlenkamp C, Galindo-Lagunas KA, Guan Z, Vinuesa P, Robinson S, Thomas-Oates J, Raetz CR, Geiger O.** 2007. The lipid lysyl-phosphatidylglycerol is present in membranes of Rhizobium tropici CIAT899 and confers increased resistance to polymyxin B under acidic growth conditions. Mol Plant Microbe Interact **20:**1421–1430. http://dx.doi.org/10.1094/MPMI-20-11-1421.
28. **Peschel A, Jack RW, Otto M, Collins LV, Staubitz P, Nicholson G, Kalbacher H, Nieuwenhuizen WF, Jung G, Tarkowski A, van Kessel KPM, van Strijp JAG.** 2001. Staphylococcus aureus resistance to human defensins and evasion of neutrophil killing via the novel virulence factor Mprf is based on modification of membrane lipids with L-lysine. J Exp Med **193:**1067–1076. http://dx.doi.org/10.1084/jem.193.9.1067.
29. **Bao Y, Sakinc T, Laverde D, Wobser D, Benachour A, Theilacker C, Hartke A, Huebner J.** 2012. Role of mprF1 and mprF2 in the pathogenicity of Enterococcus faecalis. PLoS One **7:**e38458. http://dx.doi.org/10.1371/journal.pone.0038458.
30. **Fabretti F, Theilacker C, Baldassarri L, Kaczynski Z, Kropec A, Holst O, Huebner J.** 2006. Alanine esters of enterococcal lipoteichoic acid play a role in biofilm formation and resistance to antimicrobial peptides. Infect Immun **74:**4164–4171. http://dx.doi.org/10.1128/IAI.00111-06.
31. **Fedtke I, Mader D, Kohler T, Moll H, Nicholson G, Biswas B, Henseler K, Gotz F, Zahringer U.** 2007. A Staphylococcus aureus ypfP mutant with strongly reduced lipoteichoic acid (LTA) content: LTA governs bacterial surface properties and autolysin activity. Mol Microbiol **65:**1078–1091. http://dx.doi.org/10.1111/j.1365-2958.2007.05854.x.
32. **Gross M, Cramton SE, Götz F, Peschel A.** 2001. Key role of teichoic acid net charge in Staphylococcus aureus colonization of artificial surfaces. Infect Immun **69:**3423–3426. http://dx.doi.org/10.1128/IAI.69.5.3423-3426.2001.
33. **Abachin E, Poyart C, Pellegrini E, Milohanic E, Fiedler F, Berche P, Trieu-Cuot P.** 2002. Formation of D-alanyl-lipoteichoic acid is required for adhesion and virulence of Listeria monocytogenes. Mol Microbiol **43:**1–14. http://dx.doi.org/10.1046/j.1365-2958.2002.02723.x.
34. **Powers J-PS, Hancock REW.** 2003. The relationship between peptide

structure and antibacterial activity. Peptides **24:**1681–1691. http://dx.doi.org/10.1016/j.peptides.2003.08.023.

35. **Wang L, Friesner RA, Berne BJ.** 2010. Competition of electrostatic and hydrophobic interactions between small hydrophobes and model enclosures. J Phys Chem B **114:**7294–7301. http://dx.doi.org/10.1021/jp100772w.

36. **Tanford C.** 1962. Contribution of hydrophobic interactions to the stability of the globular conformation of proteins. J Am Chem Soc **84:**4240–4247. http://dx.doi.org/10.1021/ja00881a009.

37. **Scott AM, Antal CE, Newton AC.** 2013. Electrostatic and hydrophobic interactions differentially tune membrane binding kinetics of the C2 domain of protein kinase Cα. J Biol Chem **288:**16905–16915. http://dx.doi.org/10.1074/jbc.M113.467456.

38. **Goldfine H.** 1984. Bacterial membranes and lipid packing theory. J Lipid Res **25:**1501–1507.

39. **Silhavy TJ, Kahne D, Walker S.** 2010. The bacterial cell envelope. Cold Spring Harb Perspect Biol **2:**a000414. http://dx.doi.org/10.1101/cshperspect.a000414.

40. **Ortony JH, Chatterjee T, Garner LE, Chworos A, Mikhailovsky A, Kramer EJ, Bazan GC.** 2011. Self-assembly of an optically active conjugated oligoelectrolyte. J Am Chem Soc **133:**8380–8387. http://dx.doi.org/10.1021/ja202776b.

41. **Owen DM, Rentero C, Magenau A, Abu-Siniyeh A, Gaus K.** 2012. Quantitative imaging of membrane lipid order in cells and organisms. Nat Protoc **7:**24–35. http://dx.doi.org/10.1038/nprot.2011.419.

42. **Ming X, Daeschel MA.** 1995. Correlation of cellular phospholipid con-

tent with nisin resistance of Listeria monocytogenes Scott A. J Food Prot **58:**416–420.

43. **Ming X, Daeschel M.** 1993. Nisin resistance of foodborne bacteria and the specific resistance responses of Listeria monocytogenes Scott A. J Food Prot **56:**944–948.

44. **ter Steeg PF, Hellemons JC, Kok AE.** 1999. Synergistic actions of nisin, sublethal ultrahigh pressure, and reduced temperature on bacteria and yeast. Appl Environ Microbiol **65:**4148–4154.

45. **Verheul A, Russell NJ, Van'T Hof R, Rombouts FM, Abee T.** 1997. Modifications of membrane phospholipid composition in nisin-resistant Listeria monocytogenes Scott A. Appl Environ Microbiol **63:**3451–3457.

46. **Bergstrom CL, Beales PA, Lv Y, Vanderlick TK, Groves JT.** 2013. Cytochrome c causes pore formation in cardiolipin-containing membranes. Proc Natl Acad Sci U S A **110:**6269–6274. http://dx.doi.org/10.1073/pnas.1303819110.

47. **Xu J, Vanderlick TK, Beales PA.** 2013. Lytic and non-lytic permeabilization of cardiolipin-containing lipid bilayers induced by cytochrome c. PLoS One **8:**e69492. http://dx.doi.org/10.1371/journal.pone.0069492.

48. **Israelachvili JN, Marčelja S, Horn RG.** 1980. Physical principles of membrane organization. Q Rev Biophys **13:**121–200. http://dx.doi.org/10.1017/S0033583500001645.

49. **Kumar VV.** 1991. Complementary molecular shapes and additivity of the packing parameter of lipids. Proc Natl Acad Sci U S A **88:**444–448. http://dx.doi.org/10.1073/pnas.88.2.444.

50. **Myers CR, Nealson KH.** 1988. Bacterial manganese reduction and growth with manganese oxide as the sole electron acceptor. Science **240:**1319–1321. http://dx.doi.org/10.1126/science.240.4857.1319.